

# SCIENTIFIC REPORTS



OPEN

## Association between preterm brain injury and exposure to chorioamnionitis during fetal life

Received: 22 June 2016  
Accepted: 02 November 2016  
Published: 01 December 2016

Devasuda Anblagan<sup>1,2,\*</sup>, Rozalia Pataky<sup>1,\*</sup>, Margaret J. Evans<sup>3</sup>, Emma J. Telford<sup>1</sup>, Ahmed Serag<sup>1</sup>, Sarah Sparrow<sup>1</sup>, Chinthika Piyasena<sup>4</sup>, Scott I. Semple<sup>4,5</sup>, Alastair Graham Wilkinson<sup>6</sup>, Mark E. Bastin<sup>2</sup> & James P. Boardman<sup>1,2</sup>

Preterm infants are susceptible to inflammation-induced white matter injury but the exposures that lead to this are uncertain. Histologic chorioamnionitis (HCA) reflects intrauterine inflammation, can trigger a fetal inflammatory response, and is closely associated with premature birth. In a cohort of 90 preterm infants with detailed placental histology and neonatal brain magnetic resonance imaging (MRI) data at term equivalent age, we used Tract-based Spatial Statistics (TBSS) to perform voxel-wise statistical comparison of fractional anisotropy (FA) data and computational morphometry analysis to compute the volumes of whole brain, tissue compartments and cerebrospinal fluid, to test the hypothesis that HCA is an independent antenatal risk factor for preterm brain injury. Twenty-six (29%) infants had HCA and this was associated with decreased FA in the genu, cingulum cingulate gyri, centrum semiovale, inferior longitudinal fasciculi, limbs of the internal capsule, external capsule and cerebellum ( $p < 0.05$ , corrected), independent of degree of prematurity, bronchopulmonary dysplasia and postnatal sepsis. This suggests that diffuse white matter injury begins *in utero* for a significant proportion of preterm infants, which focuses attention on the development of methods for detecting fetuses and placentas at risk as a means of reducing preterm brain injury.

Globally, preterm birth affects around 10% of deliveries and is a leading cause of neurodevelopmental impairment<sup>1</sup>. Adverse outcome is strongly associated with a phenotype that combines diffuse white matter injury and reduced connectivity of developing neural systems apparent on neonatal brain magnetic resonance imaging (MRI), with cognitive impairment and educational under-attainment in childhood<sup>2–5</sup>. This phenotype is partly explained by co-morbidities such as bronchopulmonary dysplasia (BPD)<sup>6</sup> and postnatal sepsis<sup>7</sup>, and is influenced by nutritional<sup>8</sup> and genetic factors<sup>9</sup>. Pre-clinical and epidemiological studies demonstrate a clear association between abnormal systemic inflammation at a critical point in development and preterm brain injury (for review see<sup>10</sup>).

Chorioamnionitis (infection/inflammation of the amniotic fluid, membranes, placenta and/or decidua) affects around 40–80% of very preterm deliveries and it can initiate a fetal inflammatory response that is injurious to the developing brain and other organs<sup>11,12</sup>. In meta-analyses, chorioamnionitis is associated with cystic periventricular leukomalacia and cerebral palsy in preterm infants<sup>13</sup>, but there is uncertainty about its contribution to the more common preterm phenotype (diffuse white matter injury), and its importance in relation to co-morbidities. Some of these uncertainties may be attributable to study designs that have used variable case definitions (clinical or histopathological diagnostic criteria), and many studies were conducted before the era of quantitative neonatal brain MRI for defining cerebral outcome.

Diffusion MRI (dMRI) provides objective measures of white matter microstructure in the newborn that are altered in association with preterm birth: a consistent finding is that fractional anisotropy (FA), a biomarker

<sup>1</sup>MRC Centre for Reproductive Health, University of Edinburgh, Queen's Medical Research Institute, 47 Little France Crescent, Edinburgh EH16 4TJ, UK. <sup>2</sup>Centre for Clinical Brain Sciences, University of Edinburgh, Chancellor's Building, 49 Little France Crescent, Edinburgh EH16 4SB, UK. <sup>3</sup>Department of Pathology, Royal Infirmary of Edinburgh, 51 Little France Crescent, Edinburgh, EH16 4SA, UK. <sup>4</sup>Centre for Cardiovascular Science, University of Edinburgh, Queen's Medical Research Institute, 47 Little France Crescent, Edinburgh EH16 4TJ, UK. <sup>5</sup>Clinical Research Imaging Centre, University of Edinburgh, 47 Little France Crescent, Edinburgh EH16 4TJ, UK. <sup>6</sup>Department of Radiology, Royal Hospital for Sick Children, 9 Sciennes Road, Edinburgh, EH9 1LF, UK. \*These authors contributed equally to this work. Correspondence and requests for materials should be addressed to J.P.B. (email: james.boardman@ed.ac.uk)

		Histologic Chorioamnionitis (n = 26)	No Histologic Chorioamnionitis (n = 64)	p value
Mean GA age at birth/weeks (range)		27 <sup>+6</sup> (23 <sup>+2</sup> –30 <sup>+4</sup> )	29 <sup>+4</sup> (25 <sup>+0</sup> –32 <sup>+6</sup> )	0.001
Mean birth weight/g (SD)		1088 (550–1525)	1180 (670–1635)	0.106
Mean birth weight z-score (SD)		0.17 (0.49)	−0.39 (0.94)	0.007
Mean GA at scan/weeks (range)		39 <sup>+4</sup> (38 <sup>+0</sup> –42 <sup>+2</sup> )	40 <sup>+2</sup> (38 <sup>+0</sup> –42 <sup>+5</sup> )	0.012
Mean weight z-score at scan (SD)		−0.71 (1.16)	−1.07 (1.08)	0.177
Postnatal sepsis, n (%)	Any	16 (62)	22 (36)	0.033
	Early onset*	8 (31)	7 (11)	0.031
	Late onset**	10 (38)	20 (31)	0.623
Necrotizing enterocolitis, n (%)		2 (8)	3 (5)	0.624
Gender (M:F)		12:14	34:30	0.569
BPD, n (%)		8 (31)	17 (27)	0.436
Antenatal MgSO <sub>4</sub> , n (%)		18 (69)	28 (44)	0.037
Antenatal corticosteroid, n (%)		23 (88)	45 (70)	0.104

**Table 1. Demographic and clinical features of preterm infants with and without chorioamnionitis.**

\*Postnatal sepsis <72 hours after birth; \*\*postnatal sepsis >72 hours after birth.

linked to white matter microstructure, is reduced in white matter tracts of preterm infants at term equivalent age compared with term-born matched controls<sup>14,15</sup>. Tract-based Spatial Statistics (TBSS) is a powerful unbiased method for group-wise analysis of FA images derived from dMRI data<sup>16</sup>. It has been applied to neonatal dMRI to map microstructural change in white matter tracts of preterm infants at term equivalent age<sup>17</sup>, to identify clinical risk factors for altered brain development<sup>6</sup>, to detect tissue effects of neuroprotective treatment strategies<sup>18</sup>, and it may have a role in early risk stratification because it predicts neurodevelopmental outcome<sup>2,5</sup>. Computational analysis of structural MRI data enables the calculation of brain volume (whole brain or tissue compartments) and is useful for identifying factors associated with growth deficits<sup>8,19</sup>, and for longitudinal modeling of growth in early life<sup>20,21</sup>.

We combined histologic classification of chorioamnionitis with neonatal brain MRI, and used TBSS and computational morphometry to test the hypothesis that HCA is associated with altered white matter microstructure and brain volume in preterm infants at term equivalent age.

## Results

**Patients.** Placental histopathology and brain dMRI were acquired from 90 infants born preterm: 26 (29%) had histologic chorioamnionitis and 64 (71%) had no evidence of chorioamnionitis. Table 1 summarizes the demographic and clinical details of the two groups.

Preterm infants with HCA had a lower GA at birth ( $p = 0.001$ ), and the prevalence of prolonged rupture of membranes (>24 hours before delivery) was higher in this group (69% versus 8%). The proportion of infants exposed to antenatal MgSO<sub>4</sub> for the purpose of fetal neuroprotection was greater in the HCA group: 69% versus 44% ( $p = 0.037$ ). There was no significant difference in antenatal steroid exposure between the groups. Five out of 90 participants were treated for necrotizing enterocolitis, and three required treatment for retinopathy of prematurity. Postnatal somatic growth, measured as the difference between birth weight z-score and weight at scan z-scores, did not differ significantly between the two groups: the mean difference (SD) in weight z-score for the HCA group was −0.98 (1.07) versus −0.67 (1.06) for preterm infants without HCA exposure ( $t = 1.247$ ,  $p = 0.216$ ).

**Placental histopathology.** 26 of 90 (29%) placental plates showed patterns of inflammatory reaction on the maternal side, and 20 of these showed an inflammatory response of the cord and/or the umbilical vessels. The patterns of maternal/fetal inflammation are shown in the Table 2.

**Magnetic resonance imaging.** 49 infants (54%) had abnormal white matter using the classification system described by Woodward *et al.*<sup>22</sup>, and 8 infants (9%) had punctate white matter lesions. One infant had a solitary cyst in left peritrigonal white matter (diameter 5 mm).

**White matter correlates of histologic chorioamnionitis.** The findings are provided corrected for GA at birth, GA at image acquisition, BPD and postnatal sepsis. Preterm infants exposed to HCA had decreased FA in the genu of corpus callosum, cingulum cingulate gyri, centrum semiovale, corticospinal tracts (CST), inferior longitudinal fasciculi (ILF), left arcuate, anterior and posterior limbs of internal capsule, external capsule and cerebellum (Fig. 1);  $p < 0.05$  corrected. Skeleton-wide FA was 5.3% lower in preterm infants with HCA compared to infants born without this exposure;  $p = 0.006$  (FA in the range of 0.182–0.255 for infants with HCA and 0.172–0.279 for infants without HCA exposure, respectively), (Fig. 2).

**Histologic chorioamnionitis and brain tissue volume.** Structural MRI data were available for 81 of the 90 participants; nine structural MRI data were not useable due to movement artefact. Whole brain tissue volume increased over the range of gestational age at image acquisition (Fig. 3), but there was no difference in brain tissue

Fetal inflammatory responses					Maternal inflammatory responses					
Vasculitis (Stage 1)		Vasculitis 1 or more vessels (Stage 2)		Funisitis (Stage 3)	Chorionitis (Stage1)		Chorioamnionitis (Stage2)		Necrotising chorioamnionitis (Stage 3)	Breeches the chorion-Intervillositis
1 = Yes, 0 = No	Grade	1 = Yes, 0 = No	Grade		1 = Yes, 0 = No	Grade	1 = Yes, 0 = No	Grade	1 = Yes, 0 = No	1 = Yes, 0 = No
1	1	0		0	0		1	1	0	1
0		1	2	1	0		1	2	0	1
0		1	2	1	1	1	1	2	1	1
0		0		0	1	1	0		0	0
0		1	2	1	0		1	2	1	1
1	1	0		0	1	1	0		0	1
1	2	0		1	1	2	0		0	1
0		0		0	1	1	0		0	0
0		1	1	1	0		1	2	1	1
0		1	1	1	1	1	0		0	1
0		1	2	1	0		1	2	1	0
0		1	1	1	1	2	0		0	1
0		1	2	1	1	1	0		0	1
0		1	2	1	0		1	2	1	0
0		0		0	1	1	0		0	0
0		1	1	1	0		1	1	1	1
0		1	2	1	0		1	1	0	1
0		1	1	1	0		1	2	0	1
0		1	2	1	1	2	0		1	1
0		1	1	1	0		1	2	0	0
0		0		0	1	1	0		0	0
0		0		0	1	1	0		0	1
0		0		0	1	1	0		0	0
0		1	1	1	0		1	2	0	1
0		1	1	1	0		1	1	0	1
1	1	0	0	1	0		0		0	0

**Table 2.** Patterns of inflammatory response in 26 cases with histologic chorioamnionitis.

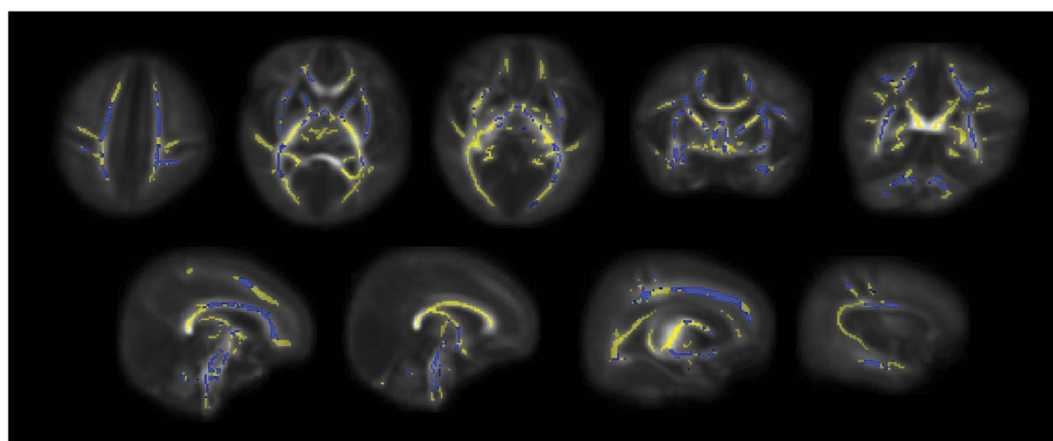


**Figure 1.** Mean FA skeleton (yellow) overlaid on the mean FA map in axial, coronal and sagittal planes. Voxels demonstrating significantly lower FA in preterm infants at term equivalent who had been exposed to HCA are overlaid in blue.

volume attributable to HCA: mean 388.9 ml (SD 44.0) for 23 infants with HCA versus mean 391.4 ml (SD 37.4) for 58 infants without the exposure. There were no significant differences in the volume of any tissue compartment or cerebrospinal fluid between the groups (Table 3).

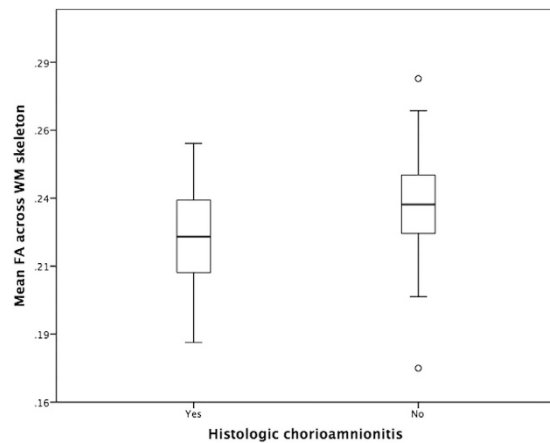


**Figure 2.** Mean FA across the white matter skeleton of preterm infants grouped by presence of histologic chorioamnionitis.

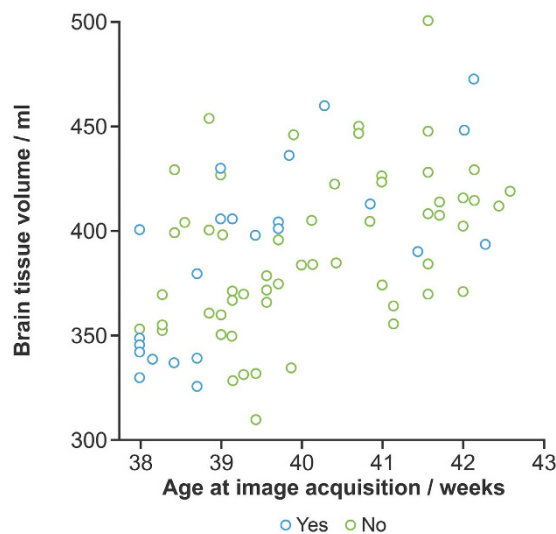


**Figure 3.** Brain tissue volume at term equivalent age for each participant colour coded by presence of HCA (blue) or absence of HCA (green).

	Mean volume (SD) / ml (histologic chorioamnionitis)	Mean volume (SD) / ml (no histologic chorioamnionitis)	<i>p</i> -value
White matter	138.8 (14.2)	138.4 (14.6)	0.70
Deep grey matter	5.2 (0.86)	5.3 (0.80)	0.19
Cortical grey matter	169.2 (24.6)	173.4 (19.7)	0.42
Cerebellum	22.7 (3.8)	24.5 (3.3)	0.06
Brainstem	5.2 (0.9)	5.2 (0.8)	0.70
Cerebrospinal fluid	79.8 (17.1)	75.6 (18.0)	0.32

**Table 3.** Mean (SD) brain tissue and cerebrospinal fluid volumes at term equivalent age.

## Discussion

By combining histological diagnosis of chorioamnionitis with quantitative brain MRI, we have shown that inflammation *in utero* contributes to altered microstructure in major white matter tracts of preterm infants at term equivalent age. The effect was independent of age at image acquisition and known predictors of preterm brain injury and poor neurodevelopmental outcome including degree of prematurity, BPD and postnatal sepsis.

Meta-analysis has shown that HCA is a significant predictor of cerebral palsy (CP)<sup>13</sup>, and HCA has been associated with intraventricular haemorrhage<sup>23</sup>, brain imaging abnormalities<sup>24</sup>, and cystic periventricular leukomalacia<sup>25</sup>. However, the role of confounding by gestational age at birth and co-morbid conditions on these associations

is unclear; and in some studies chorioamnionitis has no adverse effect on neurodevelopmental outcome<sup>26,27</sup>. Such differences may be explained by the heterogeneity of HCA, which encompasses a range of grades and stages of maternal and fetal inflammation that have variable effects on the fetal inflammatory response. A strength of this study is that 77% of infants classified as HCA-exposed had fetal vasculitis affecting the cord (funisitis) or chorionic plate, which is the histological indicator of fetal inflammatory response syndrome (FIRS) since it reflects transmigration of fetally derived neutrophils to bacteria in the amniotic fluid<sup>28</sup>.

The fetal inflammatory response is characterized by increased concentration of pro-inflammatory cytokines in plasma<sup>29</sup>. During postnatal life these mediate brain injury by several mechanisms including: increased permeability of the blood brain barrier to cytotoxic proteins<sup>30</sup>; activation of microglia<sup>31</sup>; dysmaturation of the oligodendrocyte lineage and ultimately hypomyelination<sup>32</sup>; neuronal injury and cell death<sup>33</sup>; modification of the endogenous stem cell populations<sup>10</sup>; generation of reactive oxygen and nitrogen species<sup>32</sup>; sensitization of the brain to subsequent hypoxic-ischaemic insults<sup>34</sup>; and activation of the coagulation cascade<sup>35</sup>. After delivery, systemic inflammation due to postnatal bloodstream infection or necrotizing enterocolitis is a powerful predictor of neurodisability among preterm infants<sup>7</sup>, and MRI studies suggest that the neural substrate includes injury to the white matter<sup>36,37</sup>. Our data suggest that *antenatal* exposure to systemic inflammation contributes to the prevailing form of preterm brain injury. This is consistent with a previous observation that elevated cytokines and CD45RO<sup>+</sup> T lymphocytes in umbilical cord blood are associated with overt cerebral lesions on MRI very soon after birth<sup>38</sup>. MRI acquisition in the early post-partum period after very preterm birth (around 30 weeks gestational age) is feasible and recent advances in post-processing techniques enable the evaluation of diffuse white matter injury, connectivity measures, cortical maturation and growth trajectories at this early stage<sup>39–44</sup>. These approaches could be combined with collateral biological information about fetal/maternal inflammation to investigate specific antenatal determinants of abnormal brain development.

We used TBSS to survey the white matter skeleton for group-wise differences that might be associated with HCA because of its sensitivity for detecting alterations in FA in the newborn period, and because of its predictive value for later outcome<sup>25</sup>. FA is considered a robust marker of tract microstructure that reflects fibre density, axonal diameter, wrapping by pre-myelinating oligodendrocytes and myelination. These data suggest that infants exposed to HCA have less coherently organised and more immature fibre tracts at term equivalent age compared with preterm infants without HCA-exposure. We found no difference in whole brain tissue volume, or the volumes of tissue class compartments between the groups, which is consistent with previous observations that preterm brain injury is characterized by reduced connectivity of neural systems rather than a global failure of brain growth for the majority of preterm infants<sup>19,45</sup>. BPD and intrauterine growth restriction are associated with reduced brain volumes, but the prevalence of these was similar between groups<sup>8,19</sup>. In previous work we showed that preterm infants with elevated ADC values in white matter had focal tissue volume reduction in deep grey matter nuclei compared with healthy term controls born at term<sup>46,47</sup>, but there was no difference in deep grey matter structure when the preterm group was compared with preterm infants without white matter injury. This is consistent with the findings of the current study, and may be explained by smaller differences in water diffusion parameters between preterm subgroups, compared with the differences reported between preterm infants and healthy controls<sup>17</sup>.

Our study has some limitations. Firstly, although 77% of the HCA group had fetal vasculitis, which is indicative of FIRS, we did not analyze cord blood so further study is required to uncover the specific immune mediators that might link HCA with white matter injury, and also to investigate susceptibility in infants without FIRS. Secondly, the study was not powered to investigate the role of multiple placental lesions, which could act synergistically to increase fetal risk. Thirdly, the diagnosis of neonatal sepsis is imprecise; we overcame this by using a rigorous clinical protocol that meets international bench-marking standards (Vermont Oxford Network) but it is possible that some cases were misclassified. In future, integrating quantitative imaging data with information about the host response to infection/inflammation provided by pathway analysis may offer new insights into the timing and drivers of inflammation-induced perinatal brain injury.

In conclusion, these results suggest that the pathway to white matter injury originates *in utero* for a significant proportion of preterm infants exposed to HCA during fetal life. Future research could focus on the development of antenatal tests to identify HCA and fetuses at risk of neuroinflammation; and placental histopathology may have a role in risk stratification for trials of immune-modulatory therapies designed to improve outcome.

## Methods

**Participants.** The study was conducted according to the principles of the Declaration of Helsinki, and ethical approval was obtained from the UK National Research Ethics Service (South East Scotland Research Ethics Committee). Written parental informed consent was obtained for all subjects. The cohort consisted of preterm infants born at <33 completed weeks' gestational age (GA) who received care at the Royal Infirmary of Edinburgh between July 2012 and May 2015, who underwent brain MRI at term equivalent age and whose placentas were available for histologic examination. Exclusion criteria were infants with congenital infection, chromosomal abnormalities, post-haemorrhagic ventricular dilatation, porencephalic cysts and cystic periventricular leucomalacia.

Postnatal sepsis was defined by: 1) positive blood culture growing pathogenic bacteria; *or* 2) blood cultures negative or positive for coagulase negative staphylococcus (CoNS) *plus* generalized signs of infection *plus* physician decision to treat with antibiotics for 5 days or more. BPD was defined by the requirement for supplemental oxygen at 36 weeks' GA.

Postnatal somatic growth was described in terms of change in weight z-score between birth and scan, calculated using Intergrowth-21<sup>st</sup> reference standards for preterm infants<sup>48</sup>.

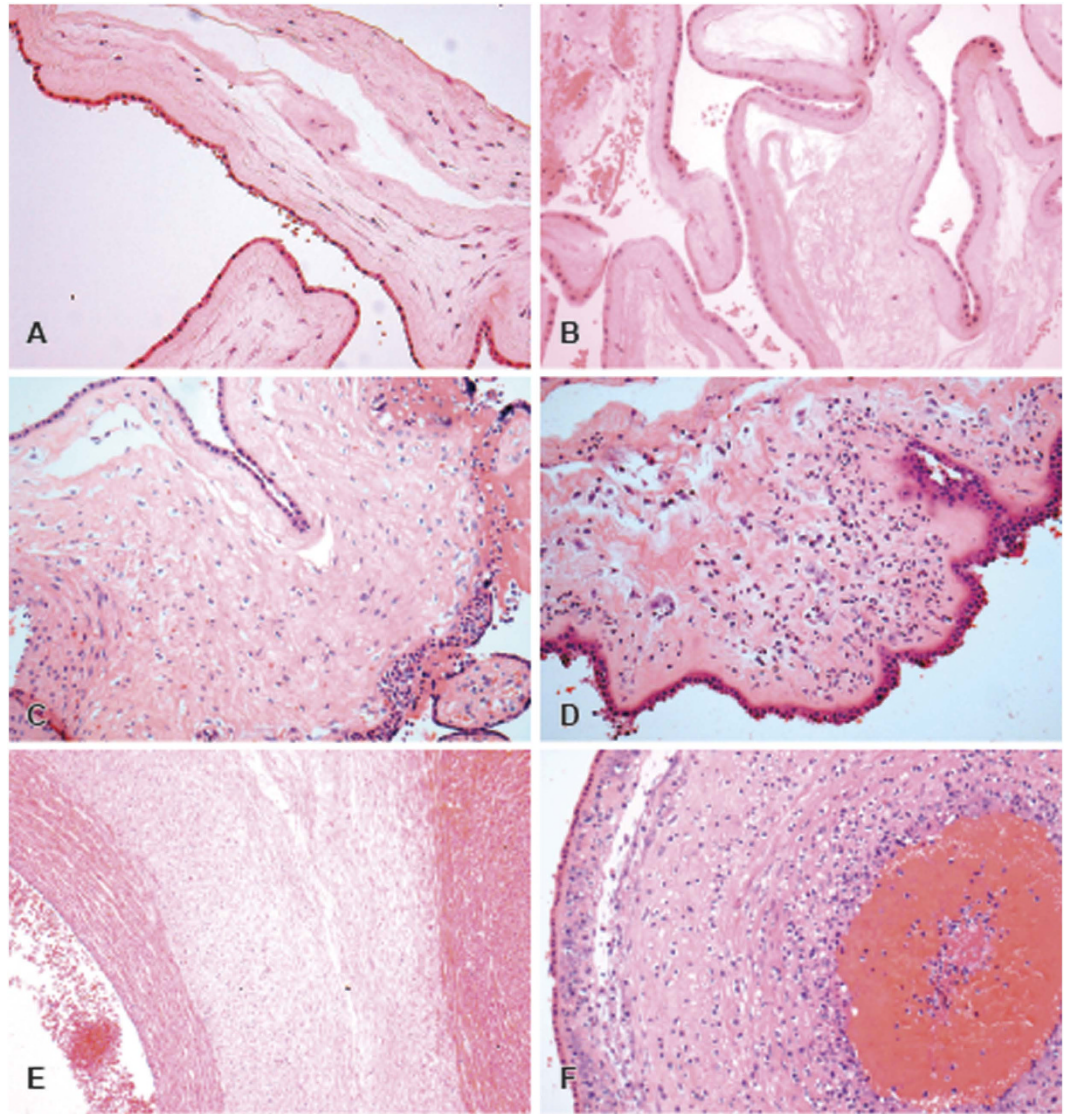


**Figure 4. Histologic features of normal membranes and reaction patterns related to maternal inflammatory response to amniotic fluid infection.** (A,B) Normal appearances of the placental membranes with no signs of inflammation. (C) Acute chorionitis (Stage 1) patchy-diffuse accumulations of neutrophils in the subchorionic plate fibrin. (D) Acute chorioamnionitis (Stage 2). Histologic features of non-inflamed cord and reaction patterns of fetal inflammatory response to amniotic fluid infection: (E) Normal appearances of umbilical vein and artery and Wharton tissue. (F) Diffuse funisitis along with umbilical vasculitis.

**Placental histopathology.** After delivery, placentae were formalin fixed and stored at 4 °C before sampling. The placentae were sampled according to a standardized protocol; distal and proximal sections of cord (the proximal section being taken at 1.5 cm from above the fetal surface), a roll of extraplacental membranes starting at the point of rupture and 4 full thickness sections from each quadrant. All were stained with Haematoxylin and Eosin. Slides were examined by a single experienced placenta pathologist (ME) with no knowledge of the MRI findings. Placental reaction patterns were reported according to site and degree of inflammation, using the structure proposed by Redline and colleagues<sup>49</sup>. The chorioamnionitis group included cases which demonstrated an inflammatory response in the placental membranes of any grade or stage, whilst the non-chorioamnionitis group demonstrated no inflammatory response. Features of normal and inflamed placental tissue are illustrated in Fig. 4.

**MRI acquisition.** MRI was performed on a Siemens Magnetom Verio 3 T system (Siemens, Healthcare GmbH, Erlangen, Germany) using a 12-channel matrix phased array head coil. All infants were scanned axially to acquire: 3D T1-weighted MPRAGE volume (~1 mm<sup>3</sup> resolution), T2-weighted STIR (~0.9 mm<sup>3</sup> resolution), T2-weighted FLAIR (~1 mm<sup>3</sup> resolution), and dMRI (11 T2- and 64 diffusion encoding direction (b = 750 s/mm<sup>2</sup>) single-shot spin-echo echo planar imaging (EPI) volumes with 2 mm isotropic voxels data, TE = 106 ms and TR = 7300 ms) data. Images were reported by a radiologist with experience in neonatal MRI (AGW).

Infants were scanned in natural sleep with monitoring of pulse oximetry, electrocardiography and temperature. A neonatal doctor and a research nurse were present during image acquisition. For ear protection, flexible earplugs and neonatal earmuffs (MiniMuffs, Natus Medical Inc., CA) were used.

Structural MRI scans were scored using the system described by Woodward *et al.*<sup>22</sup>. In summary, a white matter injury (WMI) score was calculated by adding sub-scores across 5 domains, each evaluated by a 3 point grading scale: white matter signal abnormality, periventricular white matter volume loss, presence of cystic abnormalities, ventricular dilatation, and thinning of corpus callosum. A grey matter injury (GMI) score was calculated by adding sub-scores from 3 domains: cortical abnormalities, quality of gyral maturation, and size of subarachnoid space. Therefore WMI scores ranged between 5 and 15, and GMI scores between 3 and 9. WMI scores were classified as per the original system from Woodward *et al.*<sup>22</sup>, i.e.  $\leq 6$  is normal and  $> 6$  is abnormal. GMI scores were classified as abnormal if  $\leq 4$ , and normal as  $> 4$ , using the modification described by Leuchter *et al.*<sup>50</sup>. The presence of punctate white matter lesions (high signal intensity on T1-weighted imaging and low signal on T2-weighted) was also recorded.

**Image data analysis.** *Tract-based Spatial Statistics.* dMRI data were preprocessed using FSL tools (FMRIB, Oxford, UK; <http://www.ndcn.ox.ac.uk/divisions/fmrib>). This included brain extraction, and removal of bulk infant motion and eddy current induced artifacts by registering the diffusion-weighted volumes to the first T2-weighted EPI volume for each subject. Using DTIFIT, FA maps were generated for every subject.

TBSS analysis was performed using a pipeline that was optimized for neonatal dMRI data<sup>6</sup>. An average FA map and mean FA skeleton (thresholded at  $FA > 0.15$ ) were created from the aligned data, representing the center of all white matter tracts common to both groups. Statistical comparison between groups born with and without exposure to chorioamnionitis was performed with FSL's Randomise using a general linear univariate model, with GA at birth, GA at image acquisition, BPD and postnatal sepsis listed as covariates. All FA data were subject to family-wise error correction for multiple comparisons following threshold-free cluster enhancement (TFCE) and are shown at  $p < 0.05$ <sup>51</sup>.

**Volumetric analysis.** The brain tissue was separated from non-brain tissue using an atlas-based approach<sup>21</sup>. Images were corrected for field inhomogeneity using the N4 method (<http://stnava.github.io/ANTs/>). All images from the dataset were non-linearly aligned to the 40 weeks' GA template from a neonatal brain 4D atlas<sup>52</sup>, which is the closest age-matched template to the mean age of the subjects in this study. Then, an Expectation–Maximization framework was used to segment the brain into: brainstem, cerebellum, cortex, cerebrospinal fluid, deep gray matter and white matter; where probabilistic spatial priors of each tissue were provided by the 4D atlas. Volumes were calculated for each individual tissue, and total brain tissue volume was calculated by subtracting cerebrospinal fluid from the whole brain segmentation.

**Statistics.** Student's t-test or the Mann-Whitney test was used to investigate differences in clinical and demographic variables between infants with ( $n = 26$ ) and without chorioamnionitis ( $n = 64$ ), and chi-square test or Fisher's exact test was used to compare proportions. Statistical analysis was performed using SPSS v21.0 (SPSS Inc, Chicago, IL).

## References

- Blencowe, H. *et al.* National, regional, and worldwide estimates of preterm birth rates in the year 2010 with time trends since 1990 for selected countries: a systematic analysis and implications. *Lancet* **379**, 2162–2172, doi: 10.1016/s0140-6736(12)60820-4 (2012).
- Counsell, S. J. *et al.* Specific relations between neurodevelopmental abilities and white matter microstructure in children born preterm. *Brain* **131**, 3201–3208 (2008).
- Boardman, J. P. *et al.* A common neonatal image phenotype predicts adverse neurodevelopmental outcome in children born preterm. *NeuroImage* **52**, 409–414 (2010).
- Kerr-Wilson, C. O., Mackay, D. F., Smith, G. C. & Pell, J. P. Meta-analysis of the association between preterm delivery and intelligence. *J Public Health* **34**, 209–216 (2012).
- van Kooij, B. J. *et al.* Neonatal tract-based spatial statistics findings and outcome in preterm infants. *AJNR Am J Neuroradiol.* **33**, 188–194 (2012).
- Ball, G. *et al.* An optimised tract-based spatial statistics protocol for neonates: applications to prematurity and chronic lung disease. *NeuroImage* **53**, 94–102 (2010).
- Mitha, A. *et al.* Neonatal infection and 5-year neurodevelopmental outcome of very preterm infants. *Pediatrics* **132**, e372–380, doi: 10.1542/peds.2012-3979 (2013).
- Inder, T. E., Warfield, S. K., Wang, H., Huppi, P. S. & Volpe, J. J. Abnormal cerebral structure is present at term in premature infants. *Pediatrics* **115**, 286–294 (2005).
- Boardman, J. P. *et al.* Common genetic variants and risk of brain injury after preterm birth. *Pediatrics* **133**, e1655–1663, doi: 10.1542/peds.2013-3011 (2014).
- Hagberg, H. *et al.* The role of inflammation in perinatal brain injury. *Nature Reviews Neurology* **11**, 192–208, doi: 10.1038/nrneuro.2015.13 (2015).
- Goldenberg, R. L., Culhane, J. F., Iams, J. D. & Romero, R. Epidemiology and causes of preterm birth. *Lancet* **371**, 75–84 (2008).
- Romero, R. *et al.* Sterile and microbial-associated intra-amniotic inflammation in preterm prelabor rupture of membranes. *The journal of maternal-fetal & neonatal medicine: the official journal of the European Association of Perinatal Medicine, the Federation of Asia and Oceania Perinatal Societies, the International Society of Perinatal Obstet* **28**, 1394–1409 (2015).
- Shatrov, J. G. *et al.* Chorioamnionitis and cerebral palsy: a meta-analysis. *Obstetrics & Gynecology* **116**, 387–392, doi: 10.1097/AOG.0b013e3181e90046 (2010).
- Counsell, S. J., Ball, G. & Edwards, A. D. New imaging approaches to evaluate newborn brain injury and their role in predicting developmental disorders. *Current opinion in neurology* **27**, 168–175, doi: 10.1097/wco.000000000000073 (2014).
- Anblagan, D. *et al.* Tract shape modeling detects changes associated with preterm birth and neuroprotective treatment effects. *NeuroImage: Clinical* **8**, 51–58 (2015).
- Smith, S. M. *et al.* Tract-based spatial statistics: voxelwise analysis of multi-subject diffusion data. *NeuroImage* **31**, 1487–1505 (2006).
- Anjari, M. *et al.* Diffusion tensor imaging with tract-based spatial statistics reveals local white matter abnormalities in preterm infants. *NeuroImage* **35**, 1021–1027 (2007).

18. Porter, E. J., Counsell, S. J., Edwards, A. D., Allsop, J. & Azzopardi, D. Tract-based spatial statistics of magnetic resonance images to assess disease and treatment effects in perinatal asphyxial encephalopathy. *Pediatric research* **68**, 205–209 (2010).
19. Boardman, J. P. *et al.* Early growth in brain volume is preserved in the majority of preterm infants. *Annals of Neurology* **62**, 185–192 (2007).
20. Kuklisova-Murgasova, M. *et al.* A dynamic 4D probabilistic atlas of the developing brain. *NeuroImage* **54**, 2750–2763 (2011).
21. Serag, A. *et al.* Construction of a consistent high-definition spatio-temporal atlas of the developing brain using adaptive kernel regression. *NeuroImage* **59**, 2255–2265 (2012).
22. Woodward, L. J., Anderson, P. J., Austin, N. C., Howard, K. & Inder, T. E. Neonatal MRI to predict neurodevelopmental outcomes in preterm infants. *N Engl J Med* **355**, 685–694 (2006).
23. DiSalvo, D. The correlation between placental pathology and intraventricular hemorrhage in the preterm infant. The Developmental Epidemiology Network Investigators. *Pediatric research* **43**, 15–19, doi: 10.1203/00006450-199804001-00096 (1998).
24. Leviton, A. *et al.* Maternal infection, fetal inflammatory response, and brain damage in very low birth weight infants. Developmental Epidemiology Network Investigators. *Pediatric research* **46**, 566–575 (1999).
25. Wu, Y. W. & Colford, J. M., Jr Chorioamnionitis as a risk factor for cerebral palsy: A meta-analysis. *JAMA* **284**, 1417–1424 (2000).
26. Andrews, W. W. *et al.* Early preterm birth: association between in utero exposure to acute inflammation and severe neurodevelopmental disability at 6 years of age. *Am J Obstet Gynecol* **198**, e461–e466, doi: 10.1016/j.ajog.2007.12.031 (2008).
27. Dexter, S. C. *et al.* Outcome of very low birth weight infants with histopathologic chorioamnionitis. *Obstetrics & Gynecology* **96**, 172–177 (2000).
28. Yoon, B. H. *et al.* The relationship among inflammatory lesions of the umbilical cord (funisitis), umbilical cord plasma interleukin 6 concentration, amniotic fluid infection, and neonatal sepsis. *Am J Obstet Gynecol* **183**, 1124–1129, doi: 10.1067/mob.2000.109035 (2000).
29. Gotsch, F. *et al.* The fetal inflammatory response syndrome. *Clinical obstetrics and gynecology* **50**, 652–683, doi: 10.1097/GRF.0b013e31811ebef6 (2007).
30. Stolp, H. B. *et al.* Breakdown of the blood-brain barrier to proteins in white matter of the developing brain following systemic inflammation. *Cell and tissue research* **320**, 369–378, doi: 10.1007/s00441-005-1088-6 (2005).
31. Favrais, G. *et al.* Systemic inflammation disrupts the developmental program of white matter. *Annals of Neurology* **70**, 550–565, doi: 10.1002/ana.22489 (2011).
32. Haynes, R. L. *et al.* Nitrosative and oxidative injury to premyelinating oligodendrocytes in periventricular leukomalacia. *J Neuropathol Exp Neurol* **62**, 441–450 (2003).
33. Leviton, A. & Gressens, P. Neuronal damage accompanies perinatal white-matter damage. *Trends in neurosciences* **30**, 473–478, doi: 10.1016/j.tins.2007.05.009 (2007).
34. Eklind, S. *et al.* Bacterial endotoxin sensitizes the immature brain to hypoxic–ischaemic injury. *European journal of neuroscience* **13**, 1101–1106 (2001).
35. Leviton, A. & Dammann, O. Coagulation, inflammation, and the risk of neonatal white matter damage. *Pediatric research* **55**, 541–545, doi: 10.1203/01.pdr.0000121197.24154.82 (2004).
36. Glass, H. C. *et al.* Recurrent postnatal infections are associated with progressive white matter injury in premature infants. *Pediatrics* **122**, 299–305, doi: 10.1542/peds.2007-2184 (2008).
37. Chau, V. *et al.* Postnatal infection is associated with widespread abnormalities of brain development in premature newborns. *Pediatric research* **71**, 274–279, doi: 10.1038/pr.2011.40 (2012).
38. Duggan, P. J. *et al.* Intrauterine T-cell activation and increased proinflammatory cytokine concentrations in preterm infants with cerebral lesions. *Lancet* **358**, 1699–1700 (2001).
39. Miller, S. P. *et al.* Early brain injury in premature newborns detected with magnetic resonance imaging is associated with adverse early neurodevelopmental outcome. *J Pediatr* **147**, 609–616, doi: 10.1016/j.jpeds.2005.06.033 (2005).
40. Ball, G. *et al.* Rich-club organization of the newborn human brain. *Proceedings of the National Academy of Sciences of the United States of America* **111**, 7456–7461, doi: 10.1073/pnas.1324118111 (2014).
41. Kersbergen, K. J. *et al.* Different patterns of punctate white matter lesions in serially scanned preterm infants. *PloS ONE* **9**, e108904, doi: 10.1371/journal.pone.0108904 (2014).
42. Kersbergen, K. J. *et al.* Relation between clinical risk factors, early cortical changes, and neurodevelopmental outcome in preterm infants. *NeuroImage*, doi: 10.1016/j.neuroimage.2016.07.010 (2016).
43. Makropoulos, A. *et al.* Regional growth and atlas of the developing human brain. *NeuroImage* **125**, 456–478, doi: 10.1016/j.neuroimage.2015.10.047 (2016).
44. Martinez-Biarge, M. *et al.* MRI Based Preterm White Matter Injury Classification: The Importance of Sequential Imaging in Determining Severity of Injury. *PloS ONE* **11**, e0156245, doi: 10.1371/journal.pone.0156245 (2016).
45. Ball, G. *et al.* Rich-club organization of the newborn human brain. *Proc Natl Acad Sci USA* **111**, 7456–7461 (2014).
46. Boardman, J. P. *et al.* Abnormal deep grey matter development following preterm birth detected using deformation-based morphometry. *NeuroImage*. **32**, 70–78 (2006).
47. Boardman, J. P. *et al.* A common neonatal image phenotype predicts adverse neurodevelopmental outcome in children born preterm. *NeuroImage*. **52**, 409–414 (2010).
48. Villar, J. *et al.* INTERGROWTH-21st very preterm size at birth reference charts. *Lancet* **387**, 844–845, doi: 10.1016/s0140-6736(16)00384-6 (2016).
49. Redline, R. W. *et al.* Amniotic infection syndrome: nosology and reproducibility of placental reaction patterns. *Pediatric and developmental pathology: the official journal of the Society for Pediatric Pathology and the Paediatric Pathology Society* **6**, 435–448, doi: 10.1007/s10024-003-7070-y (2003).
50. Leuchter, R. H. *et al.* Association between early administration of high-dose erythropoietin in preterm infants and brain MRI abnormality at term-equivalent age. *JAMA* **312**, 817–824, doi: 10.1001/jama.2014.9645 (2014).
51. Smith, S. M. & Nichols, T. E. Threshold-free cluster enhancement: addressing problems of smoothing, threshold dependence and localisation in cluster inference. *NeuroImage* **44**, 83–98 (2009).
52. Serag, A. *et al.* A Multi-Channel 4D Probabilistic Atlas of the Developing Brain: Application to Fetuses and Neonates. *Annals of the BMVA* **2012**, 1–14 (2012).

## Acknowledgements

We are grateful to the families who consented to take part in the study and to the nursing and radiography staff at the Clinical Research Imaging Centre, University of Edinburgh (<http://www.cric.ed.ac.uk>) who participated in scanning the infants. This work was supported by the Theirworld (<http://www.theirworld.org>) and was undertaken in the MRC Centre for Reproductive Health which is funded by MRC Centre grant (MRC G1002033). We thank Thorsten Feiweier at Siemens for collaborating with dMRI acquisitions (Works-in-Progress Package for Advanced EPI Diffusion Imaging). The supporting sources had no role in study design or collection, analysis and interpretation of data, or writing of the report. The authors report no real or potential conflicts of interest



concerning this work. JPB had full access to all of the data in the study and takes responsibility for the integrity of the data and the accuracy of the data analysis.

### Author Contributions

D.A. assisted in the design of the study, analyzed the MRI data and drafted the manuscript. M.E.B. and S.I.S. assisted in the design of the study through development of MRI acquisition protocols. R.P., E.J.T. and C.P. assisted in the design of the study through participant recruitment. M.J.E. assisted with study design and performed the histological assessment of chorioamnionitis and grading. A.S. assisted in study design and analyzed the volumetric data. A.G.W. helped design the study and clinically reported the structural MRI data. J.P.B. conceived and designed the study, analyzed the data, and drafted the final manuscript. J.P.B. takes responsibility for the integrity of the data and the accuracy of the analysis. All authors were involved in editing the final manuscript and have approved the final version.

### Additional Information

**Competing financial interests:** All co-authors have reviewed and approved the contents of the manuscript. The authors report no real or potential conflicts of interest concerning this work.

**How to cite this article:** Anblagan, D. *et al.* Association between preterm brain injury and exposure to chorioamnionitis during fetal life. *Sci. Rep.* **6**, 37932; doi: 10.1038/srep37932 (2016).

**Publisher's note:** Springer Nature remains neutral with regard to jurisdictional claims in published maps and institutional affiliations.



This work is licensed under a Creative Commons Attribution 4.0 International License. The images or other third party material in this article are included in the article's Creative Commons license, unless indicated otherwise in the credit line; if the material is not included under the Creative Commons license, users will need to obtain permission from the license holder to reproduce the material. To view a copy of this license, visit <http://creativecommons.org/licenses/by/4.0/>

© The Author(s) 2016